C.P. No. 822

C.P. No. 822

MINISTRY OF AVIATION

AERONAUTICAL RESEARCH COUNCIL

CURRENT PAPERS

The Static Pressure Distribution Around a Circular Jet Exhausting Normally from a Plane Wall into an Airstream

by

L. J. S. Bradbury and M. N. Wood

LONDON: HER MAJESTY'S STATIONERY OFFICE

1965

PRICE 7*s* 6*d* NET

U.D.C. No. 533.6.048.2 : 532.529.3

C.P. No.822

August 1964

THE STATIC PRESSURE DISTRIBUTION AROUND A CIRCULAR JET EXHAUSTING NORMALLY FROM A PLANE WALL INTO AN AIRSTREAM

by

L. J. S. Bradbury
and
M. N. Wood

SUMMARY

Measurements have been made of the static pressure distribution on the wall around a circular jet exhausting normally from one wall of a wind tunnel into the mainstream flow through the tunnel. The measurements show the way in which the pressure distributions vary with the ratio of jet to free-stream velocity and also show the regions on the wall which contribute most to the overall suction force on the wall. These overall suction forces are shown to be of the right order of magnitude to account for the lift loss observed on models of direct jet lift VTOL aircraft.

Theoretical work on the problem is briefly discussed and it is shown that a particularly simple model of the flow which has previously been suggested on a number of occasions is not really adequate.

Replaces R.A.E. Technical Note No. Aero.2978 - A.R.C. 26 392.

CONTENTS

ILLUSTRATIONS

ILLUSTRATIONS (Contd.)

1 INTRODUCTION

When a circular jet exhausts normally from the lower surface of a wing at forward speed, a pressure field is set up on the wing which invariably gives rise to a loss of lift on the wing compared to the case when the jet is absent. This phenomenon is obviously of interest in relation to the performance of direct jet lift VTOL aircraft in the transition phase of flight and has previously been studied by measuring the overall lift forces on a number of models of VTOL aircraft. This work has led to some appreciation of the importance of the ratio of jet to free-stream velocity and also of wing and jet geometries, but little of the fundamental mechanism of jet interference can be ascertained from these measurements. It was therefore decided to study in more detail the much simpler case of the aerodynamic interference between a jet exhausting normally from an infinite wall and a mainstream flow over the wall.

Experiments have been carried out in which the static pressure distribution has been measured on the wall around a jet exhausting effectively from one wall of a wind tunnel into the mainstream flow through the tunnel. Although the jet path and structure are of considerable interest in this problem, the primary object of the experiments was to observe how the pressure distributions on the wall changed with the ratio of jet to free-stream velocity and also to find which regions around the jet contributed most to the suction forces on the wall. The integrated suction forces on the wall have also been compared with direct measurements of lift loss on models of direct jet lift VTOL aircraft (Section 4.3). In addition to these principal studies, results are reported on some experiments on the effect of wall boundary layer thickness (Section 4.2), Reynolds number and pressure ratio (Section 4.4).

Theoretical work on the jet interference problem has made some progress and details of this work will be reported fully in a future note. However, a particularly simple 'solid blockage/sink entrainment' model of the flow which has been suggested on a number of occasions[6,7] is discussed in some detail in Section 5 of the present paper. It is argued that this model is not really adequate.

2 INITIAL CONSIDERATIONS

It seems relevant at the outset to consider a framework into which the experimental work can reasonably be fitted. We will consider first the case of an incompressible jet of air at ambient temperature exhausting at right angles into an airstream (velocity = U_1) from a circular orifice (radius = a) in an infinite wall (see Fig.1). It is assumed that, in the absence of the jet flow, the boundary layer on the wall would not develop appreciably over the region influenced by the jet so that it is possible to specify the boundary layer by a single thickness parameter, say the momentum thickness of this undisturbed layer. The boundary layer is also assumed to be turbulent and always of a sensibly constant profile shape. Dimensional analysis for the static pressure P on the wall gives then

$$\frac{P - P_1}{\frac{1}{2}\rho_1 U_1^2} = \text{function of } \left(\frac{r}{a}, \psi, \frac{P_J - P_1}{\frac{1}{2}\rho_1 U_1^2}, \frac{U_1 \theta}{\nu_1}, \frac{U_1 a}{\nu_1} \right) \qquad (1)$$

where P_1 and P_J are the free-stream static and jet supply pressure respectively. ρ_1 and ν_1 are the air density and kinematic viscosity respectively and r and ψ are cylindrical co-ordinates defined as shown in Fig.1. However, if the Reynolds numbers are sufficiently large, we may expect the flow to become independent of the Reynolds numbers and we may then write

$$C_P = \frac{P - P_1}{\frac{1}{2}\rho_1 U_1^2} = f\left(\frac{r}{a}, \psi, \frac{P_J - P_1}{\frac{1}{2}\rho_1 U_1^2}, \frac{\theta}{a} \right) \qquad (2)$$

In cases of practical interest, θ/a is of order 0.1 say, so that the dependence of the pressure coefficient C_P on this parameter is probably weak over the range of values normally encountered in practical problems of jet interference.

It is also to be noted that in this incompressible flow $P_J - P_1 = \frac{1}{2}\rho_J' U_J'^2$ where ρ_J' and U_J' are the jet density and velocity if the jet had exhausted to free-stream static pressure. Naturally, because the jet is both 'cold' and incompressible, $\rho_J' = \rho_1$ and $\frac{P_J - P_1}{\frac{1}{2}\rho_1 U_1^2} = \left(U_J'^2 / U_1^2 \right)$. If the jet flow is compressible or at a different temperature from the free-stream, the above dimensional arguments are more complicated. However, intuitively, we might expect for a given nozzle size that the jet path and the induced flow around it would depend primarily on the momentum flux ratio, $\rho_J' U_J'^2 / \rho_1 U_1^2$ and, therefore, equation (2) would still be valid provided we replace the parameter $\frac{P_J - P_1}{\frac{1}{2}\rho_1 U_1^2}$ by $\frac{\rho_J' U_J'^2}{\rho_1 U_1^2}$. Here the results of some experiments by Ricou and Spalding[1] are relevant since it was found that the mass flow entrained into axi-symmetric jets exhausting into stationary air depended only on the jet momentum flux irrespective of the jet density.

We may conclude these dimensional arguments by re-stating the simplest resulting relationship between the various parameters, namely

$$C_P = f\left(\frac{r}{a}, \psi, \frac{\rho_J' U_J'^2}{\rho_1 U_1^2} \right) \qquad (3)$$

To proceed beyond the dimensional arguments leading to equation (3), it is necessary to make further assumptions about the nature of the flow.

Since no exact method of solution is possible, a simplified tractable model of the flow must be constructed. Some consideration to this problem will be given in Section 5.

The overall suction force on the wall can be represented in two ways. On the one hand, we may define a suction force coefficient given by

$$C_S = \frac{\text{Suction force}}{\frac{1}{2}\rho_1 U_1^2 \pi a^2} = -\frac{1}{\pi}\int_0^{2\pi}\int_1^{r/a} C_P \frac{r}{a}\, d\left(\frac{r}{a}\right) d\psi \qquad (4)$$

which is roughly analogous with a negative lift coefficient on a wing. Alternatively, we may present the results in the form of the ratio of the suction force, S, on an area of the wall to the thrust, T_J, from the jet if it exhausted isentropically to free-stream static pressure. This ratio is related to the suction force coefficient by

$$\frac{S}{T_J} = \frac{1}{2}\frac{\rho_1 U_1^2}{\rho_J' U_J'^2} C_S \qquad (5)$$

3 MODEL DETAILS

The experimental programme was carried out during the latter months of 1962 in the No.1 $11\frac{1}{2}$ ft × $8\frac{1}{2}$ ft low speed wind tunnel at R.A.E. Farnborough. The apparatus, shown in Fig.2, consisted of a platform 6 ft × 7 ft which stood 3.5 inches above the tunnel floor and from which the jet exhausted normally into the mainstream. The centre section of the platform comprised a Tufnol sheet preceded by a pad of porous plastic material mounted flush with the surface. Some control over the boundary-layer thickness at the position of the jet exit was obtained by applying suction to the porous surface. Suction was provided by a 3 h.p. two stage centrifugal fan capable of removing approximately 300 cu ft of air per minute against a pressure of 30 inches of water. This was just adequate for the purpose of the experiment.

The jet exhausted through a 1 inch diameter orifice at the centre of a Tufnol disc (diameter = 16.75 inches) which had a radial row of 15 static holes. A complete picture of the surface pressure distribution could thus be obtained by rotating the disc. The static pressures were measured on two banks of inclined manometers. Near the jet, where the pressures were largest, ordinary inclined manometers were used, but pressures at the disc edge were measured on a bank of special inclined manometers developed by Bryer at the N.P.L. which could be used for accurate measurement at angles as low as 1^o. All manometers were calibrated against a standard Betz manometer before and after test runs.

The jet was supplied from a 3 inch diameter pipe via a short contraction. Since the length of parallel 1 inch diameter pipe preceding the jet exit was only 2.5 inches, the theoretical isentropic mass flow and momentum flux obtained from the measured stagnation pressure should not differ from the actual values by more than 5% (see, for example, Wood[2]).

Pressure gradients over the wall in the undisturbed mainstream flow were quite negligible. The static pressure coefficients were obtained by measuring the difference in static pressure at any point with and without the jet flow.

4 EXPERIMENTAL RESULTS

4.1 Scope of tests

The experiments consisted of the following tests.

(i) At U_1 = 60 ft/sec, some static pressure measurements were made along radial lines at 0°, 90° and 180° to the free-stream direction at different values of the boundary layer parameter, θ/a, to assess the effects of this parameter. These tests were carried out with $\sqrt{\frac{P_J - P_1}{\frac{1}{2}\rho_1 U_1^2}}$ = 2, 4 and 8. Tests were also carried out with a 3 ft long 1 inch diameter circular cylinder inserted into the jet orifice.

(ii) At U_1 = 60 ft/sec and $\theta/a \approx 0.3$, measurements of static pressure all round the jet with $\sqrt{\frac{P_J - P_1}{\frac{1}{2}\rho_1 U_1^2}}$ = 2, 4, 8 and 12 and with the circular cylinder, enough points being taken to evaluate the pressure integral given as equation (4) in Section 2.

(iii) With U_1 = 60 ft/sec and 120 ft/sec, static pressure measurements were made along radial lines at 0°, 90° and 180° to the free-stream direction with nine values of $\sqrt{\frac{P_J - P_1}{\frac{1}{2}\rho_1 U_1^2}}$ ranging from 2 to 12 and also with the circular cylinder. The purpose of these tests was to observe the effects of Reynolds number and Mach number.

(iv) With U_1 = 0, the static pressures on the wall due to jet entrainment alone were measured.

(v) Some flow visualisation tests on the wall surrounding the jet were made.

4.2 The effect of boundary layer thickness

In Fig.3 are shown the boundary layer profiles, together with the respective values of the displacement thickness δ^* and momentum thickness θ encountered in the tests. The suction facilities limited the tests to a minimum value of $\theta/a \approx 0.3$ at 120 ft/sec and the majority of the later tests were carried out with this boundary layer thickness even at 60 ft/sec.

Figs.4 and 5 show the pressure distributions along radial lines at 0°, 90° and 180° to the free-stream direction for the flow around a circular cylinder and a jet with $U_J'/U_1 = 8$ and for three values of θ/a. The free-stream velocity was 60 ft/sec in these tests. There is clearly a measurable effect of the parameter θ/a but these effects are detailed rather than gross. It seems reasonably certain therefore that the main features of the pressure distributions with $\theta/a \approx 0.3$ are representative of pressure distributions obtained with practical values of θ/a*. Although second order differences of uncertain magnitude must be expected, they should not be so large as to invalidate any of the main conclusions of the present work.

4.3 The pressure distributions and overall suction forces

As mentioned in Section 2, it is necessary to form a model of the flow if theoretical work is to proceed beyond simple dimensional arguments. One of the simplest ideas that has been suggested on a number of occasions is to assume that if $U_J' >> U_1$ then the jet can be replaced, as far as the pressures on the wall are concerned, by a semi-infinite circular cylinder. Under these circumstances, equation (3) becomes simply

$$C_p = \text{function of } (\frac{r}{a}, \psi) \text{ only} \qquad (6)$$

and the suction force coefficient takes on a constant value. It was with this simple idea in mind that the static pressure distribution around a circular cylinder was included in the present experiments. However, from Figs.7 to 11 which show in polar form lines of constant static pressure coefficient around a circular cylinder and jet with $U_J'/U_1 = 2$, 4, 8 and 11.3** respectively, it is apparent that the simple circular cylinder analogy is inadequate. Not only do the static pressure distributions around the jet differ from that around the circular cylinder but they also differ from one another thus showing a strong dependence on the parameter U_J'/U_1. In consequence, some alternative to the simple idea discussed above must be found and aspects of this problem are discussed later in Section 5. It is also relevant to compare the pressure distribution around a circular cylinder obtained from potential flow theory (Fig.6) with the measured distribution (Fig.7). Clearly, there is not much similarity between the two distributions downstream of an angle, ψ, of about 45°.

---

*Values of θ/a for practical jet lift installations are roughly in the range from, say, 0.02 to 0.2.

**Because the flow in the bulk of the tests was essentially incompressible no distinction has been made between U_J'/U_1 and $\sqrt{\rho_J' U_J'^2/\rho_1 U_1^2}$. However, compressibility effects are beginning to have an effect for $\sqrt{\frac{P_J - P_1}{\frac{1}{2}\rho_1 U_1^2}} = 12$ at $U_1 = 60$ f.p.s. and the value of $U_J'/U_1 = 11.3$ actually refers to the square root of the momentum flux ratio rather than the velocity ratio as suggested in the text.

Also, of course, the measured static pressure at the front of the cylinder does not reach stagnation pressure because of boundary layer effects.

As a first step towards calculating the overall suction force coefficients, C_S, the integral $\int_1^{r/a} C_P \frac{r}{a} d(\frac{r}{a})$ was evaluated from the experimental results at the various stations around the jet for values of r/a of 5, 10 and 15. The distributions of this integral for the circular cylinder and the four jet velocity ratios studied are shown in Fig.12 which may be thought of as showing the contribution to the overall suction force coefficient per unit angle around the jet. It can be seen that the angular region which makes the major contribution to the suction force coefficient moves forward (i.e. upstream) with increasing jet velocity.

The overall suction force coefficients were obtained from Fig.12 by finding the area under the respective curves (c.f. equation (4)) and the resulting values are shown in Fig.13. The main feature of these results is that, for the larger values of U_J'/U_1, the suction force coefficient shows an ever decreasing dependence on U_J'/U_1. For example, for r/a = 5 and $U_J'/U_1 \geq 4$, the suction-force coefficient takes on an apparently constant value of about 11. In the case of r/a = 10, the suction force coefficient appears to be roughly constant at a value of about 25 for $U_J'/U_1 \geq 8$. In the case of r/a = 15, although the suction force coefficient has not attained a constant value even at $U_J'/U_1 = 11.3$, it would appear to be following similar trends to the other two values of r/a. However, it should be recalled that the pressure coefficient fields giving rise to the apparently constant values of the suction force coefficient are not themselves unchanging (see Figs.8 to 11). Thus, although the suction force coefficients may appear constant, the pitching moment coefficients, for example, are not.

Integrated lift losses from the present results can usefully be compared with direct measurements of lift loss on a direct jet lift VTOL model. In Fig.14 values of the parameter S/T_J from the present experiments are compared with values obtained by Wood[3] on a simple model comprising a single jet in a fuselage with a small delta wing. The forces on the finite wing and on a comparable area over the infinite wall seem to be very similar. This suggests that, for the area ratios encountered, the lift loss on finite wings occurs primarily as a result of a pressure field on the lower surfaces of the wing which may not be very different from that found on the infinite wall. However, until static pressure measurements become available on finite wings, it is not possible to be sure about this point.

4.4 The Reynolds number and pressure ratio effects

A few tests were carried out in which the pressure distribution directly upstream of the jet at $\psi = 0^\circ$ was measured for a wide range of jet speeds at two tunnel speeds of 60 ft/sec and 120 ft/sec. The boundary layer thickness was constant at $\theta/a \approx 0.3$ for both tunnel speeds. Although these tests were

not comprehensive, they showed that there was only a very small effect of the two fold increase in Reynolds number and, in the case of compressible jets, it seems that comparison of pressure distributions on the basis of a momentum flux ratio, $\rho_J' U_J'^2/\rho_1 U_1^2$, as suggested in Section 2, is not unreasonable. In order to obtain more substantive results over a wider range, some further work on these aspects is planned. With regard to the Reynolds number effect, it can be argued that, provided both the jet flow and wall boundary layer are turbulent, the Reynolds number effect may reasonably be expected to be small. The suggestion that some critical Reynolds number effect similar to that found for flow around a circular cylinder may occur[7] seems quite untenable on physical grounds.

4.5 Flow patterns

Although a detailed investigation of the flow structure was not undertaken, a few simple flow visualisation tests were made on the wall surrounding the jet. The results of these tests for the circular cylinder and $U_J'/U_1 = 2$, 4 and 8 are shown in Fig.15. In each case $\theta/a \approx 0.3$. A region of separated flow at the front of the jet is visible and the extent of this region apparently diminishes with increasing jet speed. This is consistent with the reduction in the severity of the adverse pressure gradients at the front of the jet found with increasing jet speed. Also of interest is the "sink" effect of the jet which is causing the flow streamlines to turn in behind the jet. The precise cause of the curious flow pattern downstream of the jet, particularly with $U_J'/U_1 = 8$, is unknown but the most likely explanation is that it is a region in which the wall boundary layer is separating and being drawn up into the jet. Support for this idea comes from the work of Jordinson[8] and a few isolated measurements in the present experiments in which it was found that the total head of the flow behind the jet was less than the free-stream total head even several jet diameters above the wall. It has been suggested that this low total head region is simply the wake of the free-stream flow past the jet but it is difficult to imagine how the jet flow with a total head higher than the free-stream value can cause a reduction in the free-stream total head. It seems more likely that the low total head is caused by wall boundary layer air being drawn up into the jet as suggested.

Some observations of the flow with a tuft did not reveal anything unexpected. The most marked feature of the flow are the two contra-rotating vortices to either side of and slightly below the jet and which are apparent in the measurements of Jordinson[8].

5 SOME ASPECTS OF THEORETICAL MODELS OF THE FLOW

The simple circular cylinder analogy with the jet has already been shown to be inadequate (Section 4.3). However, before discarding such a concept completely, some elaboration seemed worthwhile by representing the jet by a constant geometry blockage rather than a simple circular cylinder together with a line distribution of sinks along the axis of the blockage simulating the entrainment into the jet. It will be shown in this section that even with these refinements, this model still does not seem adequate but the analysis is nevertheless worth discussion to illustrate the difficulties and failings

of this approach to the problem. Brief details of an alternative and quite different model which has had a greater measure of success are given at the end of this section.

In the 'blockage plus sinks' representation of the jet, the constant geometry blockage is still assumed to be perpendicular to the free-stream direction in view of the restriction to high values of U_J'/U_1 but it is not now assumed to be parallel sided in the way that a circular cylinder is. Since the constant geometry blockage term alone would give rise to a constant static pressure coefficient field, it is necessary to check the validity of the flow model by showing that the observed changes in the static pressure coefficient field with velocity ratio arise from the entrainment into the jet as simulated by the line sink distribution. We will begin by considering some of the basic consequences of the proposed model. The resultant velocity of the potential flow adjacent to the wall may be written

$$\vec{U} = \vec{U}_B + \vec{U}_S \tag{7}$$

$\vec{U}_B$ is the velocity vector due to the blockage and free-stream flow, $\vec{U}_S$ is the velocity vector due to the line sink distribution and will be directed radially inwards towards the jet orifice and will also be radially symmetric such that

$$\frac{|\vec{U}_S|}{U_J} = \text{function of } \left(\frac{U_J}{U_1}, \frac{r}{a}\right) \tag{8}$$

Now, the static pressure coefficient can be written as

$$C_P = 1 - \frac{|\vec{U}|^2}{U_1^2} = 1 - \frac{|\vec{U}_B|^2}{U_1^2} - \frac{|\vec{U}_S|^2}{U_1^2} - 2\,\frac{|\vec{U}_B|\;|\vec{U}_S|\cos\beta}{U_1^2} \tag{9}$$

where β is the angle between the velocity vector $\vec{U}_B$ and $\vec{U}_S$. Substituting this expression into equation (4) for the suction force coefficient gives

$$C_S = C_{S_B} + C_{S_S} \tag{10}$$

where C_{S_B} is the suction force coefficient due to the constant geometry blockage alone - which is a constant - and C_{S_S} is the suction force coefficient due to the line sink distribution alone - which will depend on the velocity ratio, U_J'/U_1.

When the velocity ratio, U_J'/U_1, becomes very large, the entrainment into the jet will approach that of a jet exhausting into a stationary atmosphere

and will therefore tend to become independent of the velocity ratio. Since the constant geometry blockage argument is restricted to large values of U_J'/U_1, we may as a first estimate of the entrainment function re-write equation (8) simply as

$$\frac{|\vec{U}_S|}{U_J} = f(\frac{r}{a}) \text{ only} \tag{11}$$

where the function $f(r/a)$ can be determined from the entrainment properties of a jet exhausting into a stationary atmosphere. In Appendix 1 a semi-empirical analysis is given in which this entrainment function is determined and in Fig.18 it is shown along with some experimental results that will be discussed shortly.

In equation (9), the angle β between the velocity vectors $\vec{U}_B$ and $\vec{U}_S$ is, in general, unknown because no form for the blockage term has yet been given. But when $\psi = 0^o$ (i.e. directly upstream of the jet) $\beta = 0^o$ also and we may write for the static pressure coefficient

$$C_P = 1 - \frac{(|\vec{U}_B| + |\vec{U}_S|)^2}{U_1^2}$$

or, using equation (11) for the sink velocity, $|\vec{U}_S|$,

$$\sqrt{1 - C_P} = \frac{U_J}{U_1} f(\frac{r}{a}) + \frac{|\vec{U}_B|}{U_1} \tag{12}$$

Since the 'blockage' is assumed to be independent of U_J'/U_1, the equation (12) shows that a simple test of the above ideas is provided by plotting values of $\sqrt{1 - C_P}$ against velocity ratio, U_J'/U_1, for different values of r/a. If the flow model has any validity, these graphs should be linear for large values of U_J'/U_1 with slopes equal to the local value of the function $f(r/a)$ and intercepts with the $\sqrt{1 - C_P}$ axis equal to $|\vec{U}_B|/U_1$. It will be recalled that for $\psi = 0^o$, static pressures were obtained for values of U_J'/U_1 ranging from 2 to roughly 12 and some of these results are plotted in Fig.17 in the form suggested by the equation (12). For large values of U_J'/U_1 the experimental results are apparently in rough accord with the expected linear form, though the results are not sufficiently accurate to give very reliable values of either $|\vec{U}_B|/U_1$ or the function $f(r/a)$. Nevertheless, the comparison in Fig.18 between these experimental values of the function $f(r/a)$ with those obtained theoretically for still air ($U_1 = 0$) from the analysis of Appendix 1 shows that the experimental values are at least of the right order of magnitude.

Also shown in Fig.18 are experimental values of the function $f(r/a)$ obtained from static pressure measurements with $U_1 = 0$ (i.e. jet exhausting into a stationary atmosphere). Under these circumstances, the static pressure field arises solely from the entrainment into the jet and it is easy to show that

$$C_{P_J} = \frac{P - P_1}{\frac{1}{2}\rho_J' U_J'^2} = \frac{|\vec{U}_S|^2}{U_J'^2} = f^2\left(\frac{r}{a}\right)$$

The agreement between these experimental results and the analysis of Appendix 1 is again quite reasonable in view of the difficulties attendant in the measurements of very small static pressures.

From the preceding arguments, therefore, it seems so far that the concept of the constant geometry blockage plus sinks representation of the jet is not unreasonable. The problem of defining the constant geometry blockage term must now be resolved. The suction force coefficient over circular areas due to the sink distribution alone may be written

$$C_{S_S} = 2\left(\frac{U_J'}{U_1}\right)^2 \int_1^{r/a} f^2\left(\frac{r}{a}\right) \frac{r}{a}\, d\left(\frac{r}{a}\right)$$

Then, using the values of the function $f(r/a)$ obtained from the analysis of Appendix 1, we obtain the values of C_{S_S} given in the following table

r/a	$\int_1^{r/a} f^2(\frac{r}{a})\, d(\frac{r}{a}) \times 10^4$	C_{S_S}
5	33.3	$0.0066\ (U_J'/U_1)^2$
10	57.8	$0.0116\ (U_J'/U_1)^2$
15	75.7	$0.0152\ (U_J'/U_1)^2$

Now, according to equation (10), the overall suction force coefficient is the arithmetic sum of the suction force coefficient due to the blockage alone, C_{S_B}, and the suction force coefficient due to the sinks alone, C_{S_S}. By reference to Fig.13 and the table of values of C_{S_S}, the contribution to the overall suction force coefficient from the entrainment is seen to be very small. Consequently the overall suction force coefficient must result almost entirely from the blockage term and the fact that it is roughly constant for large values of U_J'/U_1 would seem to be additional evidence in favour of the proposed model. However, the difficulty with the model really comes when we

attempt to determine a suitable constant geometry blockage. The obvious choice of a circular cylinder is easily disposed of because the suction force coefficients obtained from measurements around a circular cylinder give the values of 2.94, 3.99 and 4.54 for values of r/a of 5, 10 and 15 respectively. By comparison with the observed values around the jet, these are much too small. Potential flow theory for flow around a circular cylinder gives

$$C_S = 1 - a^2/r^2$$

so that $C_S \to 1$ as $r/a \to \infty$ which again is far too small. Therefore, simple ideas on the blockage are not adequate and the problem arises of determining a blockage made up of a distribution of doublets, say, which gives reasonable values for the suction force coefficients and yet which is also physically realistic. Unfortunately, there is no tangible starting point for this search and little progress in this direction has so far been made. Furthermore, purely on intuitive grounds, it is difficult to imagine a physically realistic blockage giving suction force coefficients many times larger than a circular cylinder flow and, in spite of a number of points in its favour, it would seem that an approach to the problem along the lines discussed is not satisfactory.

Finally, it should be pointed out that an alternative and quite different approach to the jet interference problem has been made by P.T. Wooler[4]. It seems that this approach might prove more realistic and future papers are to be published on its development.

6 CONCLUSIONS

The simple but precise experiments described in this Note have revealed extensive low pressure regions on the plane wall surrounding a circular jet exhausting normally into a mainstream flow, particularly to the sides of the jet. The suction forces which are generated are of the right order of magnitude to account for the loss in aerodynamic lift which has been measured on complete models of simple aircraft configurations with a single lifting jet. This suggests that, for the area ratios encountered in the present Note, the lift loss may come primarily from a modification to the wing lower surface pressure distribution and that the latter may differ little from the distribution found on the infinite wall.

The angular region which makes the major contribution to the suction force on the wall depends on the ratio of the jet to the free-stream velocity. For example, at a velocity ratio of 2, the major contribution comes from an angular region from 90° to 180° to the free-stream direction, whereas at a velocity ratio of 11.3, the pattern has been effectively pulled upstream and the important region is from 30° to 120°.

The representation of the jet by an equivalent constant geometry blockage with a line distribution of sinks to simulate entrainment has been investigated. Although there is a measure of qualitative agreement between this model and the experimental results, it is shown that difficulties arise when an attempt is made to obtain quantitative agreement and these difficulties are such as to cast some doubt on the adequacy of the model.

SYMBOLS

P	static pressure
P_1	free-stream static pressure
P_J	jet supply pressure
U_1	free-stream velocity
U_J'	jet velocity when exhausting to free-stream static pressure
ρ_1	density of free-stream air
ρ_J'	jet density when exhausting to free-stream static pressure
ν_1	kinematic viscosity of free-stream air
ψ	angle defined in Fig.1
r	radius from jet nozzle centre
a	radius of jet nozzle
C_P	static pressure coefficient based on free-stream dynamic head
θ	boundary layer momentum thickness
C_S	suction-force coefficient
S	suction-force on an area of wall
T_J	jet thrust when exhausting to free-stream static pressure
$\vec{U}_B$	velocity vector due to a constant geometry blockage
$\vec{U}_S$	velocity vector due to the sink distribution

REFERENCES

No.	Author	Title, etc.
1	Ricou, F.P. Spalding, D.B.	Measurements of entrainment by axisymmetrical turbulent jets. J. of Fl. Mech. Vol.11. 1961
2	Wood, M.N.	Comparative thrust measurements on a series of jet flap configurations and circular nozzles. ARC CP 616. January 1962

REFERENCES (Contd)

No.	Author	Title, etc.
3	Wood, M.N.	Unpublished M.O.A. Report. 1962
4	Wooler, P.T.	Lift and moment forces due to a jet ejected from the lower surface of a wing. Unpublished English Electric Report
5	Laurence, J.C.	Intensity, scale and spectra of turbulence in mixing region of a free subsonic jet. NACA Report 1292. 1956
6	Vogler, R.D.	Surface pressure distribution induced on a flat plate by a cold air jet issuing perpendicularly from the plate and normal to a low speed free-stream flow. NASA T.D.1629. March 1963
7	Goldsmith, R.H. Hickey, D.H.	Characteristics of aircraft with lifting fan propulsion systems for VSTOL. IAS Paper 63-27. 1962
8	Jordinson, R.	Flow in a jet directed normal to the wind. ARC R.& M. 3074. October 1956
9	Hurn, A.G. Akers, G.A.	Notes on the effect of a jet emerging from a surface in the presence of a mainstream flow. Boulton Paul Aircraft Ltd. Technical Note No.5

APPENDIX 1

REPRESENTATION OF ENTRAINMENT INTO AN AXI-SYMMETRIC JET BY A LINE DISTRIBUTION OF SINKS

The flow of an axi-symmetric jet exhausting into a stationary atmosphere can usefully be considered as comprising two regions, namely (a) a potential core region near the jet nozzle and (b) a fully turbulent region further downstream - see Fig.16(a). The entrainment in these two regions must then be formulated.

(a) The potential core region

$$\text{Mass flow in the jet, } M = 2\pi\rho \int_0^\infty Ur\, dr$$

$$= \pi r_c^2 \rho U_J + 2\pi\rho \int_{r_c}^\infty Ur\, dr \qquad (A1)$$

where r_c is the co-ordinate of the innermost edge of the free-mixing layer. The velocity profile in the mixing layer is assumed to be everywhere similar and may be written in the form

$$U = U_J f(\eta) \qquad (A2)$$

where $f(\eta)$ is a universal function of $\eta = (r - r_c)/\delta_{0.5}$ where $\delta_{0.5}$ is the value of $(r - r_c)$ at which $U = U_J/2$.

Substituting equation (A2) into (A1) gives

$$\frac{M}{M_o} = \left(\frac{r_c}{a}\right)^2 + 2\left(\frac{\delta_{0.5}}{a}\right)^2 \int_0^\infty \eta f\, d\eta + 2\,\frac{r_c\,\delta_{0.5}}{a^2} \int_0^\infty f\, d\eta \qquad (A3)$$

where M_o is the mass flow of the jet at the nozzle. In a two-dimensional free-mixing layer, the shear layer spreads linearly with distance downstream, x. For convenience, therefore, we will also assume that

$$\frac{r_c}{a} = \left(1 - \alpha\frac{x}{a}\right) \; ; \; \frac{\delta_{0.5}}{a} = \beta\frac{x}{a} \qquad (A4)$$

where α and β are constants. Using equation (A4) in (A3) gives

$$\frac{M}{M_o} = \left(1 - \alpha\frac{x}{a}\right)^2 + 2\beta^2\left(\frac{x}{a}\right)^2 \int_0^\infty \eta f\, d\eta + 2\beta\frac{x}{a}\left(1 - \alpha\frac{x}{a}\right) \int_0^\infty f\, d\eta \qquad (A5)$$

Values must next be assigned to α and β and a form for the function $f(\eta)$.

The velocity profile function can reasonably be assumed to be

$$f(\eta) = \exp(-0.6932\,\eta^2) \tag{A6}$$

since this is known to be in good agreement with experimental results, even though the use of this function and the linear rate of spread of the mixing layer can be shown to be inconsistent with the conservation of momentum. The momentum integral equation is

$$U_J^2\,\pi a^2 = 2\pi \int_0^\infty U^2 r\,dr \tag{A7}$$

and this condition is satisfied near to the nozzle exit where $\delta_{0.5} << a$ when

$$\frac{\alpha}{\beta} = \int_0^\infty f^2\,d\eta = 0.755$$

By contrast, the momentum integral equation at the end of the potential core requires that

$$\frac{\alpha}{\beta} = \sqrt{2\int_0^\infty \eta f^2\,d\eta} = 0.85$$

By taking an average value of $\alpha/\beta = 0.8$, the calculated entrainment should be sufficiently accurate for present purposes in spite of the failure to conserve momentum throughout the potential core region. From experimental results of Laurence[5] and others, it appears that the potential core disappears at a distance downstream from the jet nozzle of about $x/a = 10$. Therefore, we may take $\alpha = 0.1$ and $\beta = 0.125$. Insertion of these values of α and β and the form of the function $f(\eta)$ given by equation (A6) gives in equation (A5)

$$\frac{M}{M_o} = 1 + 0.0658\,\frac{x}{a} + 0.00596\,\left(\frac{x}{a}\right)^2 \tag{A8}$$

and the strength of the line sink distribution to simulate entrainment in the potential core region is given by

$$\frac{dM}{dx} = \frac{M_o}{a}\,(0.0658 + 0.01192\,\frac{x}{a}) \tag{A9}$$

(b) The fully turbulent region

In order to obtain the appropriate line sink distribution to simulate entrainment in the fully turbulent region of the jet, it would be possible to carry out an analysis similar to that used for the potential core region.

However, we may use an expression obtained by Ricou and Spalding[1] from experimental results, namely that

$$\frac{M}{M_o} = 0.16\left(\frac{x}{a} - \frac{x_o}{a}\right) \tag{A10}$$

where x_o is an apparent origin of the flow in the fully turbulent region of the jet. The strength of the line sink distribution simulating entrainment in the fully turbulent region of the jet is given by

$$\frac{dM}{dx} = 0.16\,\frac{M_o}{a} \tag{A11}$$

(c) The induced velocities

From the preceding arguments, we see that the line sink distribution simulating the entrainment is similar to that shown in Fig.16. Up to the end of the potential core region at x_c/a, say, the strength of the sink distribution may be represented by

$$\frac{dM}{dx} = \frac{M_o}{a}\left(A + B\,\frac{x}{a}\right) \tag{A12}$$

where A and B are constants (c.f. equation (A9)). For $x/a \geq x_c/a$, we have a line sink distribution of constant strength,

$$\frac{dM}{dx} = C\,\frac{M_o}{a} \quad \text{(c.f. equation (A11))} \tag{A13}$$

where C is a constant. In the plane of the jet nozzle, this sink distribution and its mirror image gives rise to an induced velocity directed radially inwards towards the jet and given by

$$\frac{U_S}{U_J} = \frac{C}{2\frac{r}{a}}\left(1 - \frac{x_c}{\sqrt{x_c^2 + r^2}}\right) + \frac{A}{2\frac{r}{a}}\frac{x_c}{\sqrt{x_c^2 + r^2}} + \frac{B}{2}\left(1 - \frac{r}{\sqrt{x_c^2 + r^2}}\right) \tag{A14}$$

Using the values of A, B and C and x_c/a given by equation (A9) and (A11) leads to

$$\frac{U_S}{U_J} = \frac{0.08}{r/a}\left(1 - \frac{10}{\sqrt{100 + (r/a)^2}}\right) + \frac{0.0329}{r/a}\,\frac{10}{\sqrt{100 + (r/a)^2}} + 0.00596\left(1 - \frac{r/a}{\sqrt{100 + (r/a)^2}}\right) \tag{A15}$$

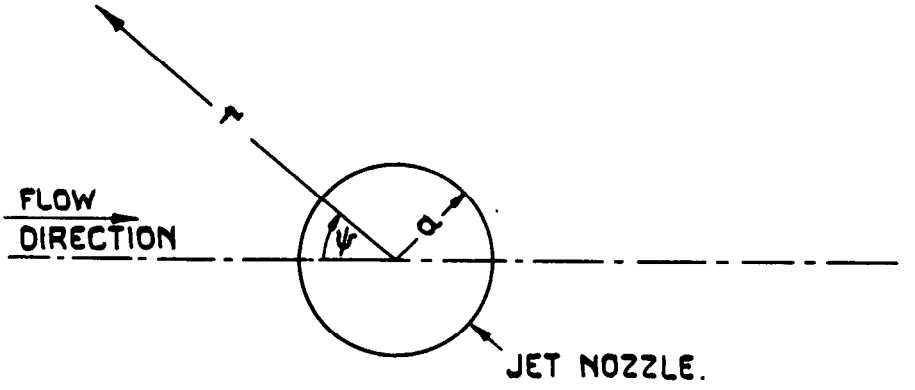

(a) PLAN VIEW.

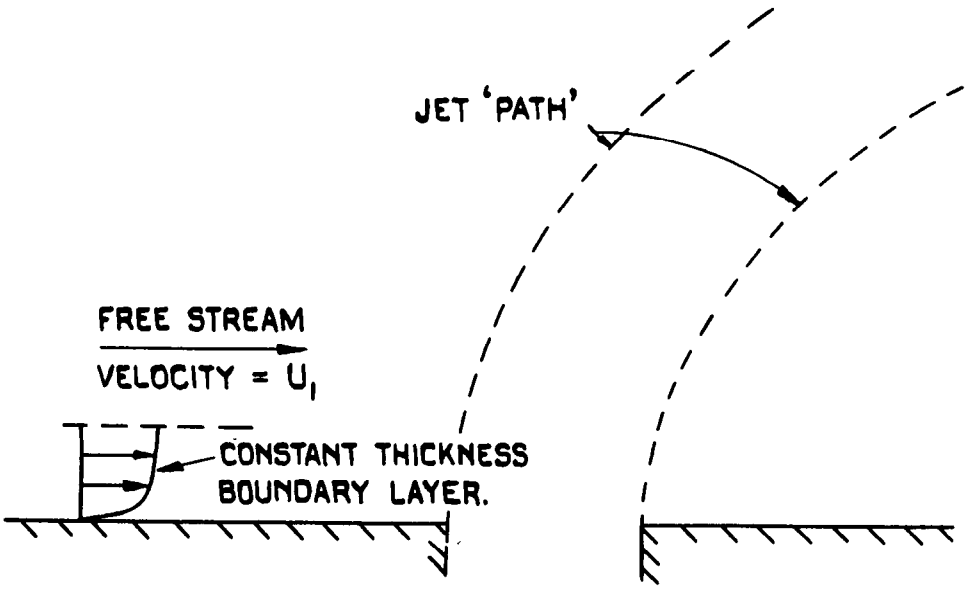

(b) SIDE VIEW.

FIG. 1. SCHEMATIC REPRESENTATION OF THE FLOW.

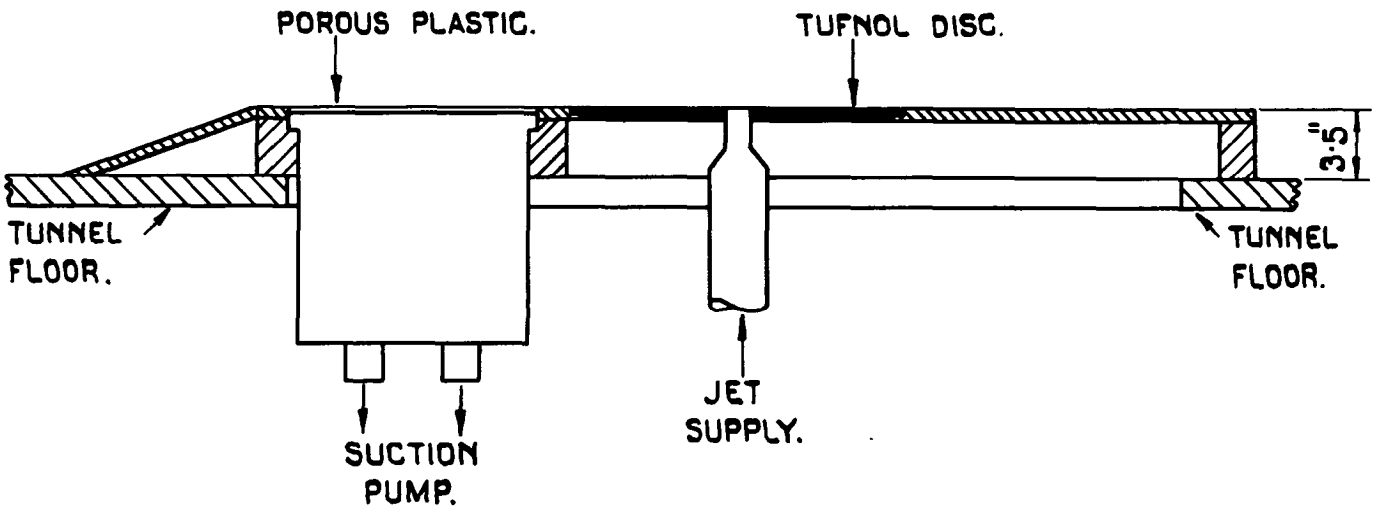

(a) CROSS SECTION THROUGH ℄.

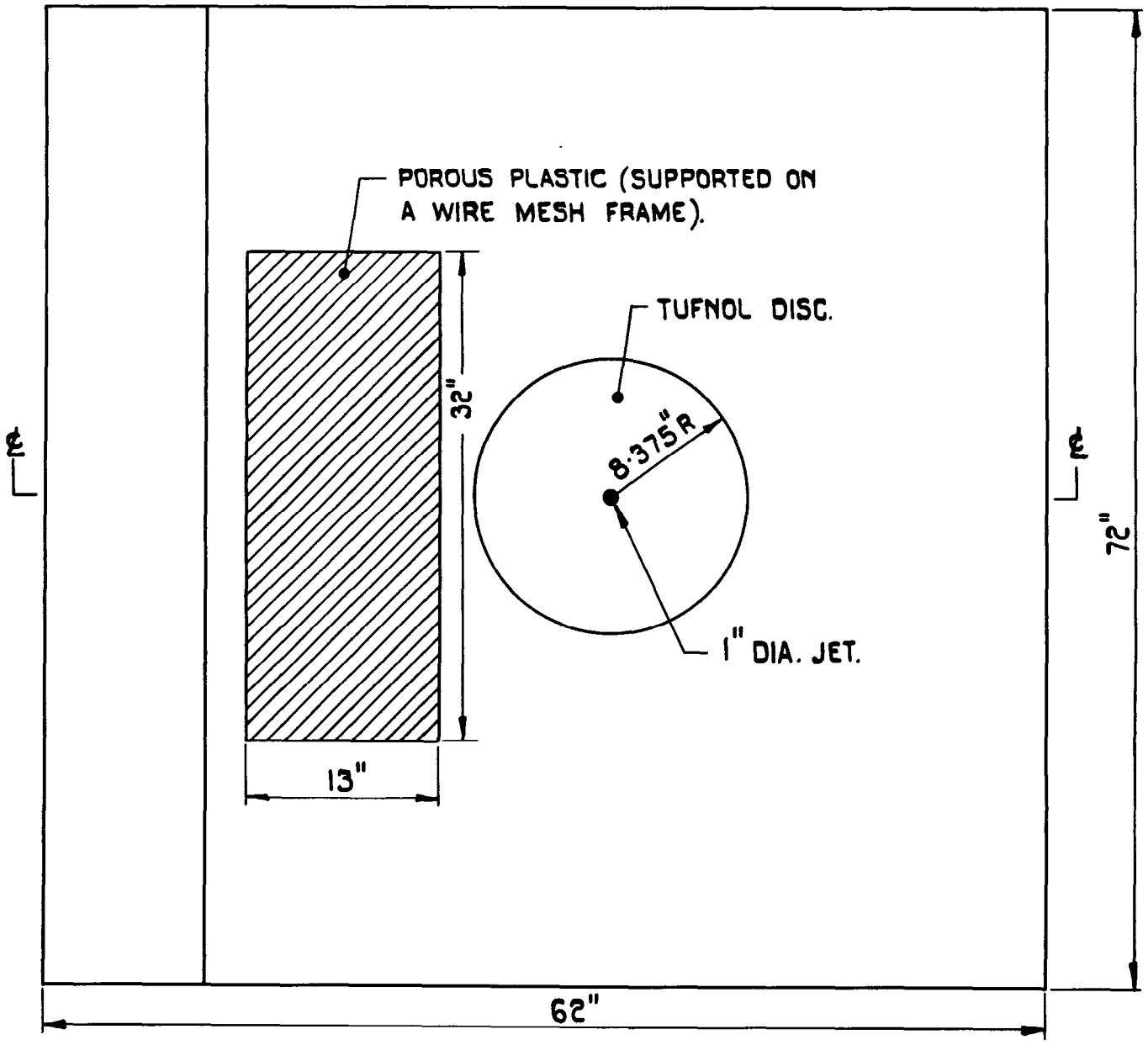

(b) PLAN VIEW.

FIG. 2. THE MODEL.

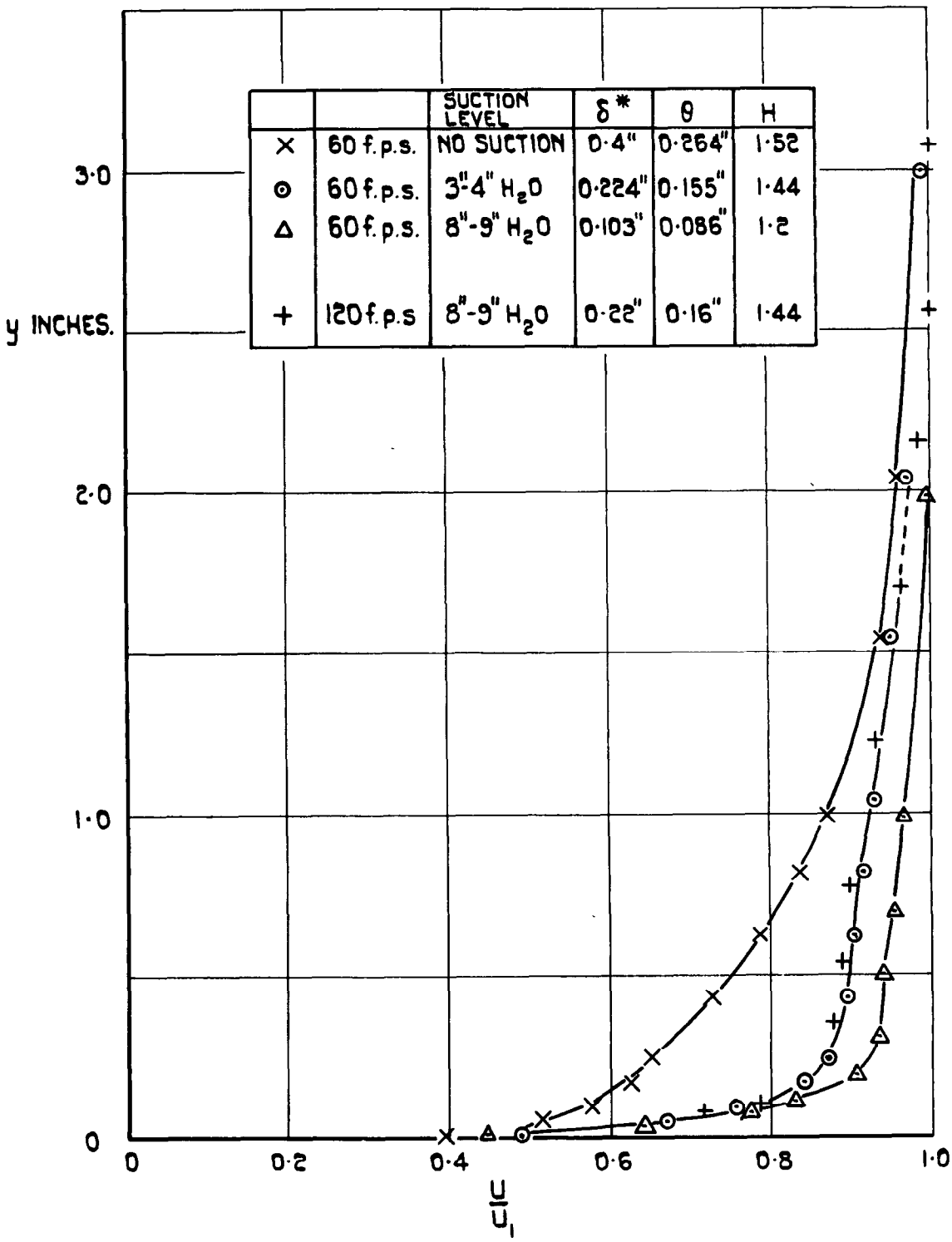

FIG. 3. BOUNDARY LAYER PROFILES FOR VARIOUS SUCTION LEVELS.

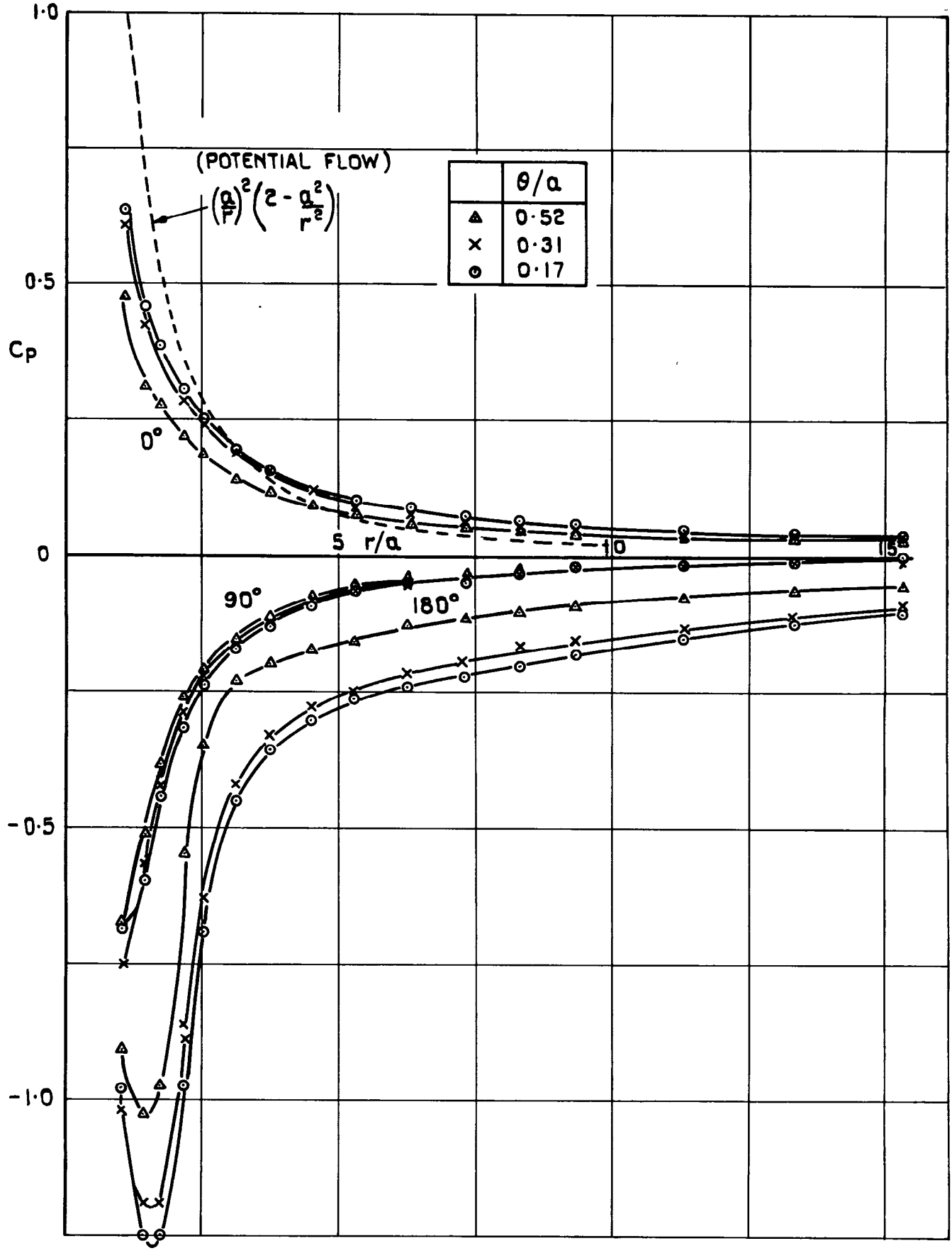

FIG. 4. EFFECT OF BOUNDARY LAYER THICKNESS ON THE PRESSURE DISTRIBUTION AROUND THE CIRCULAR CYLINDER.

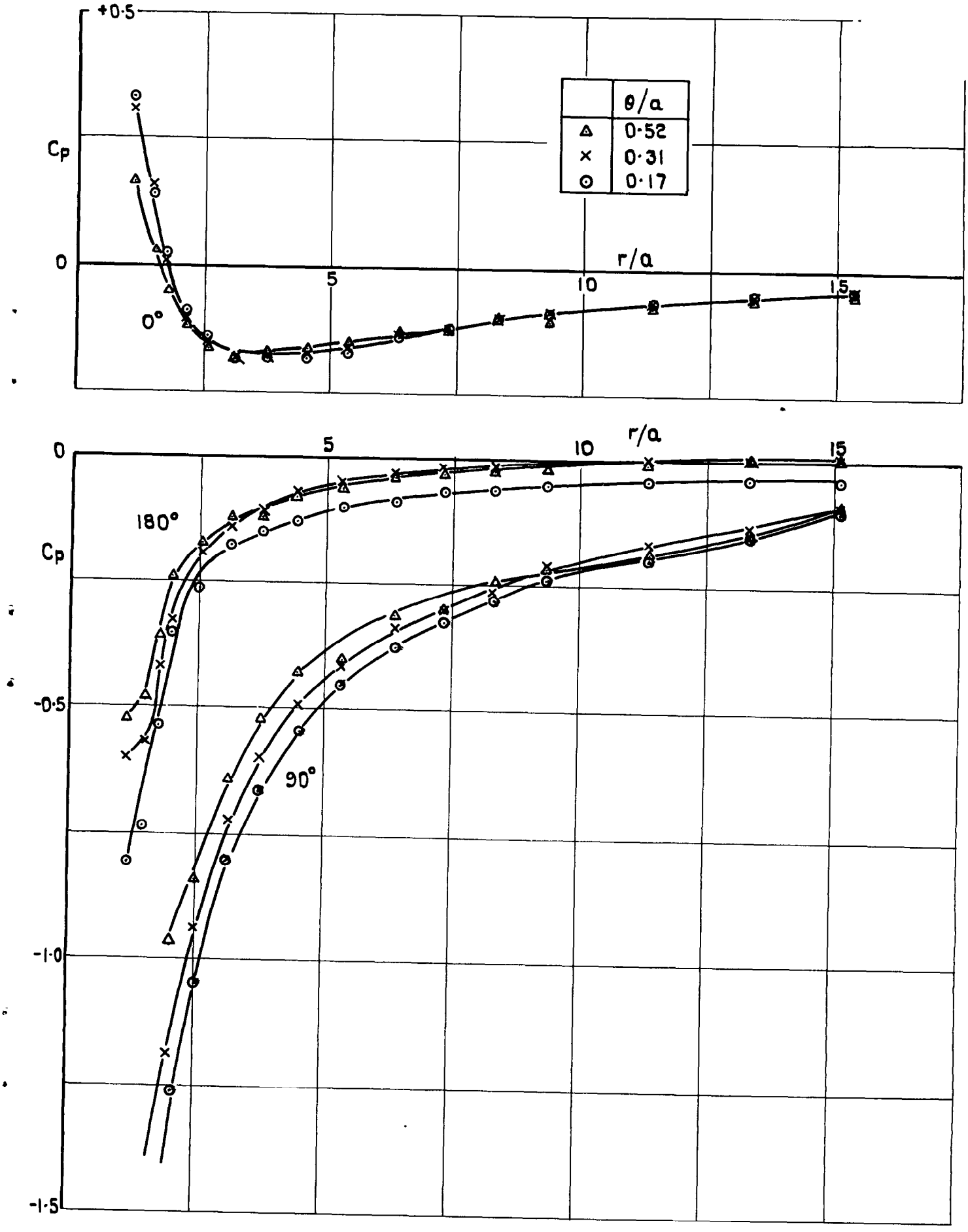

FIG. 5. EFFECT OF BOUNDARY LAYER THICKNESS ON THE PRESSURE DISTRIBUTION AROUND A JET WITH $\sqrt{\frac{P_J - P_1}{\frac{1}{2}\rho_1 U_1^2}} = 8$

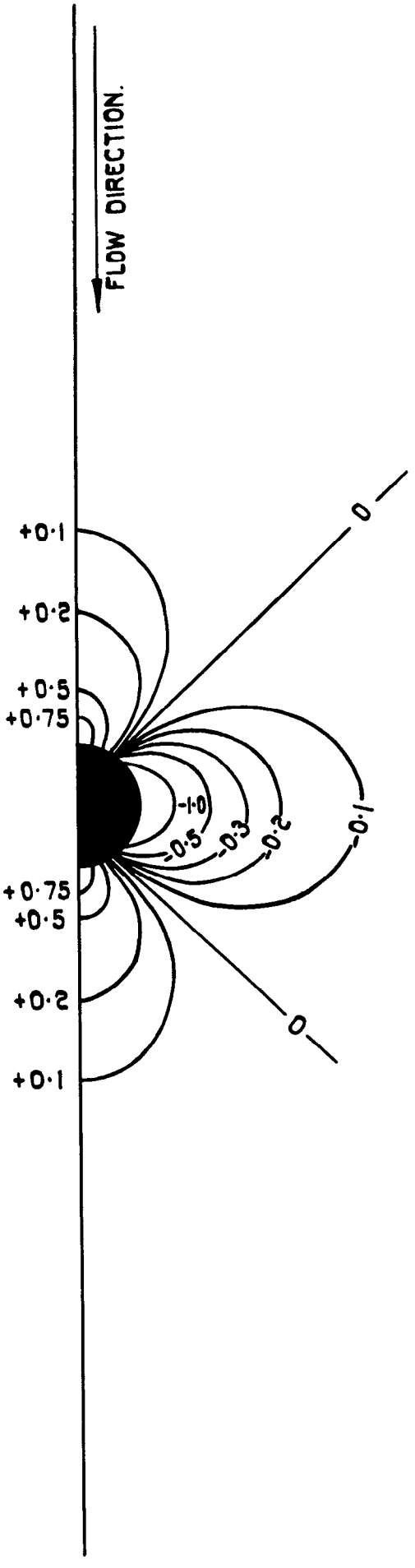

FIG. 6. PRESSURE DISTRIBUTION AROUND A CIRCULAR CYLINDER IN POTENTIAL FLOW.

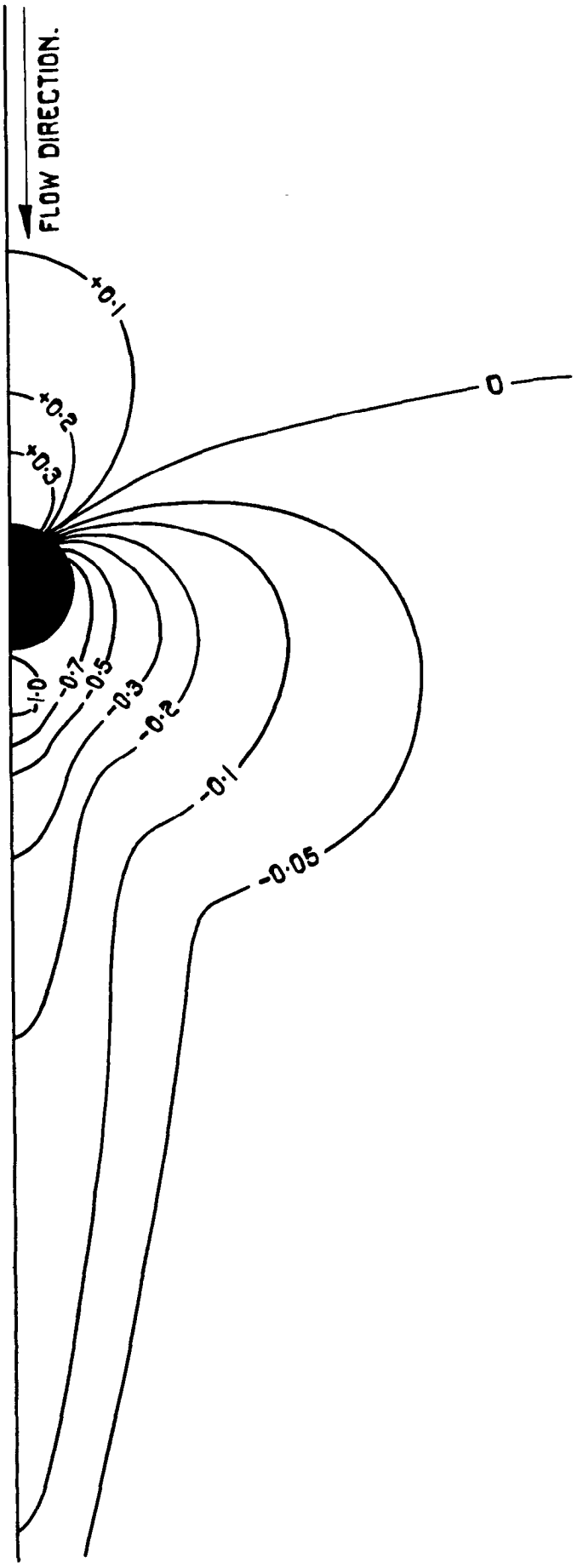

FIG. 7. PRESSURE DISTRIBUTION AROUND A CIRCULAR CLYINDER.

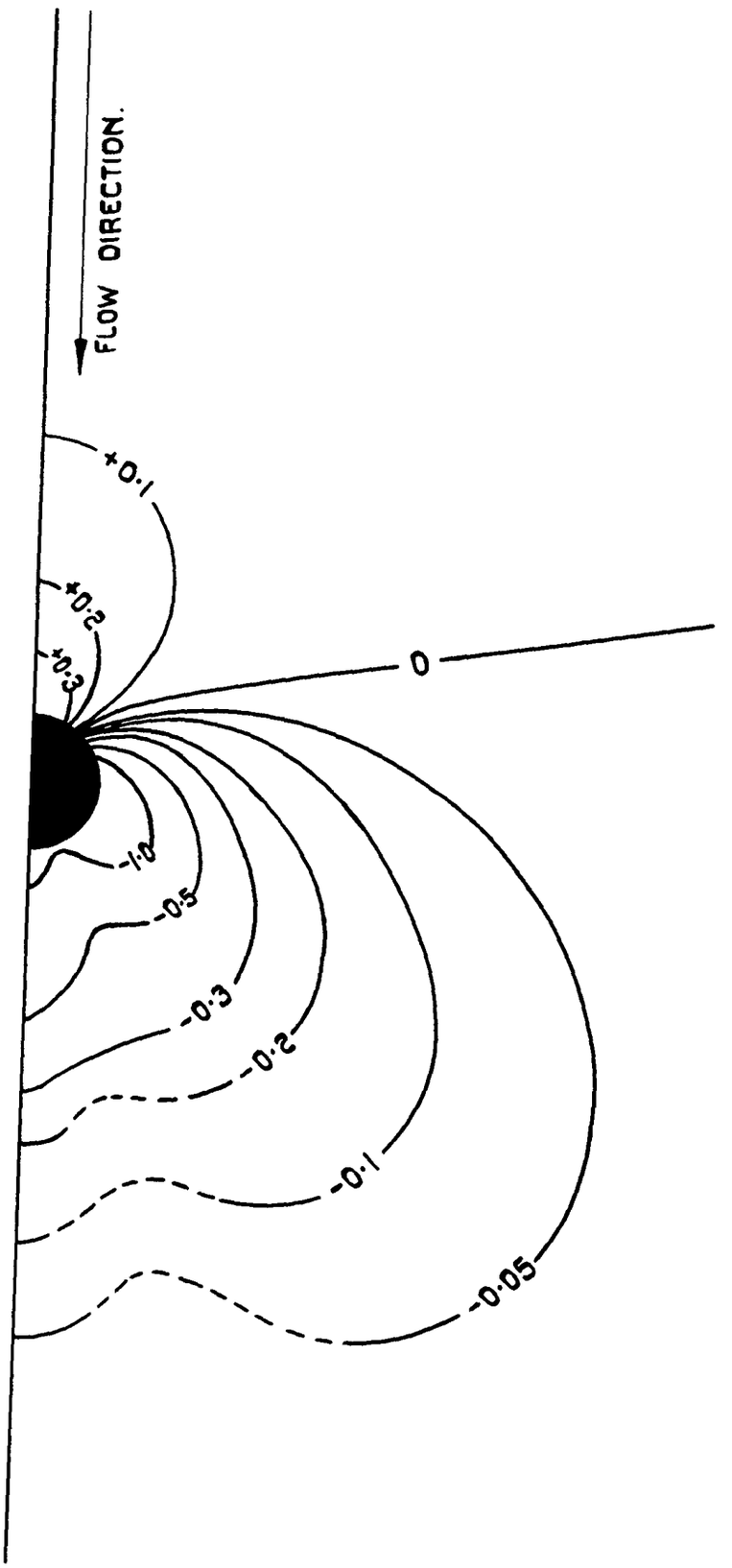

FIG. 8. PRESSURE DISTRIBUTION AROUND A CIRCULAR JET WITH $U_J'/U_1 = 2$.

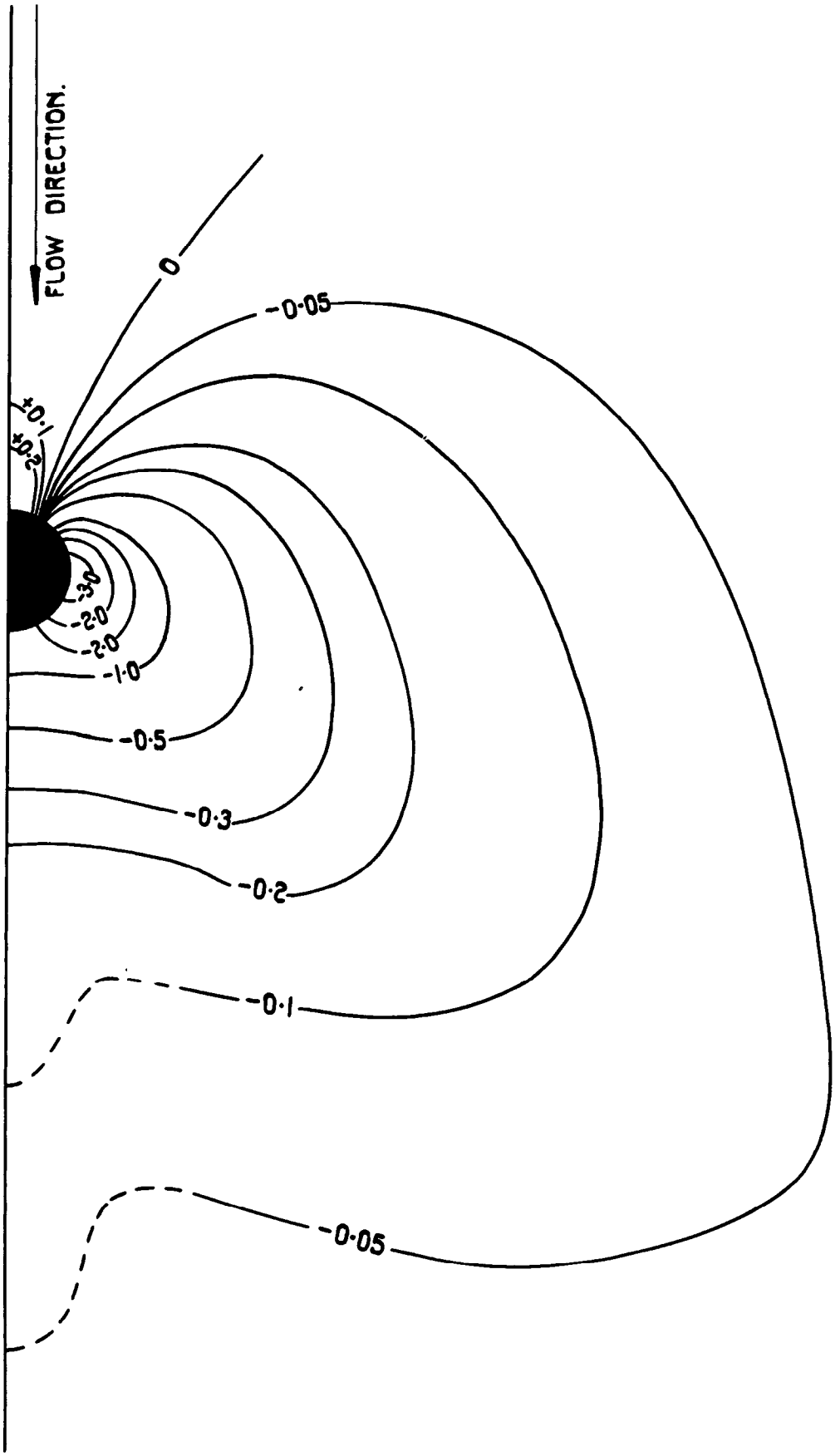

FIG. 9. PRESSURE DISTRIBUTION AROUND A CIRCULAR JET WITH $U_J'/U_1 = 4$.

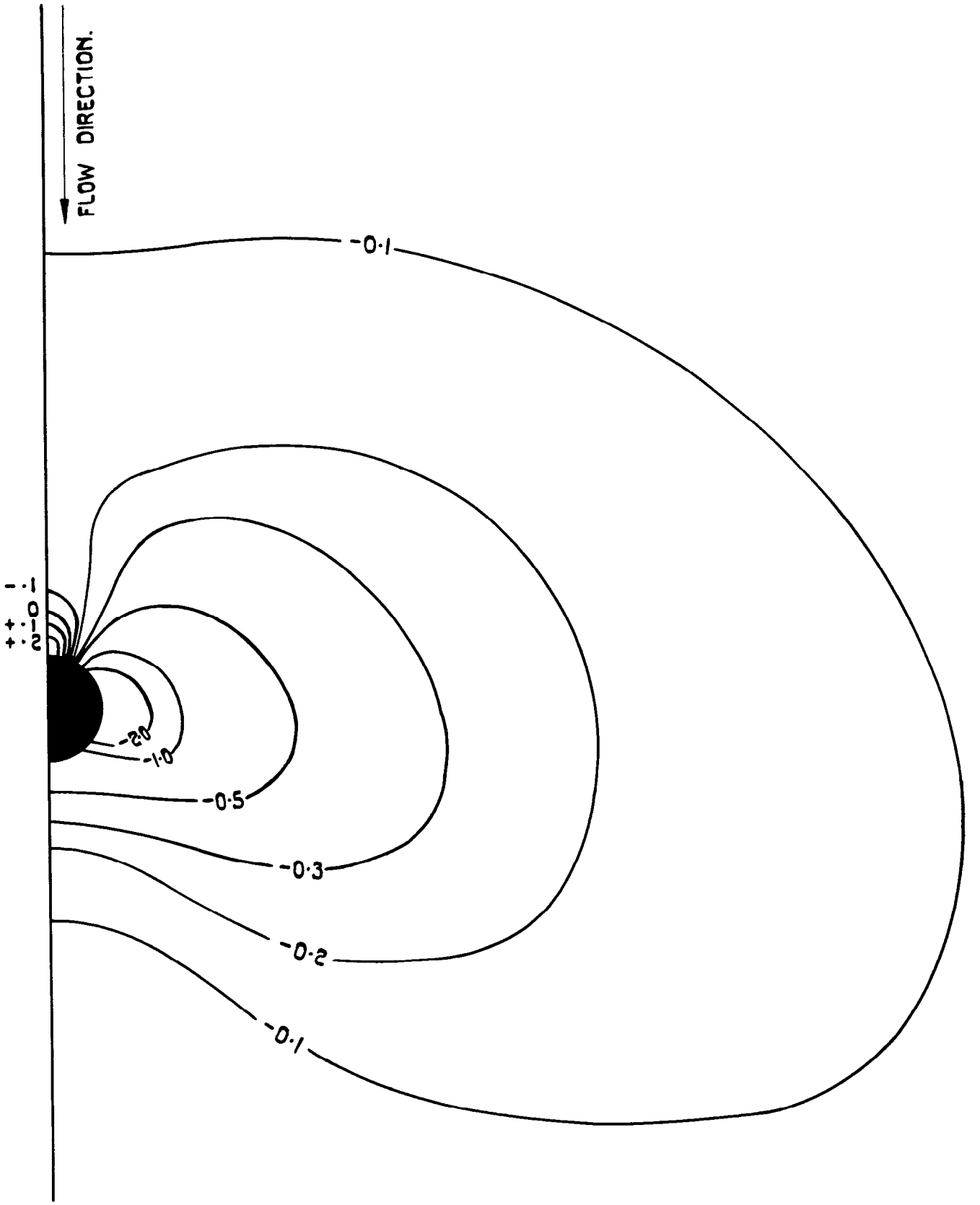

FIG. 10. PRESSURE DISTRIBUTION AROUND A CIRCULAR JET WITH $U_J'/U_1 = 8$.

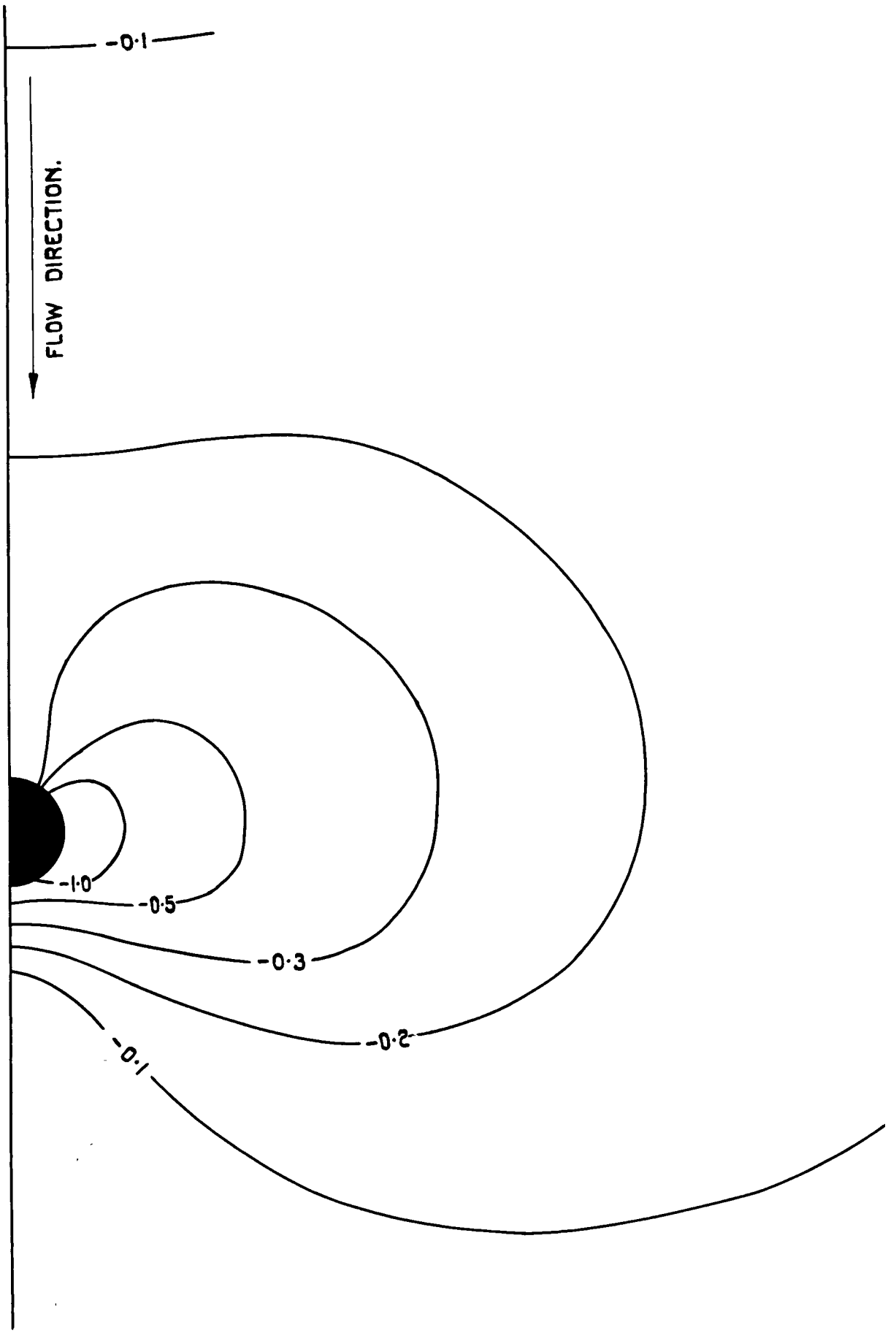

FIG. 11. PRESSURE DISTRIBUTION AROUND A CIRCULAR JET WITH $U_J'/U_1 = 11{\cdot}3$.

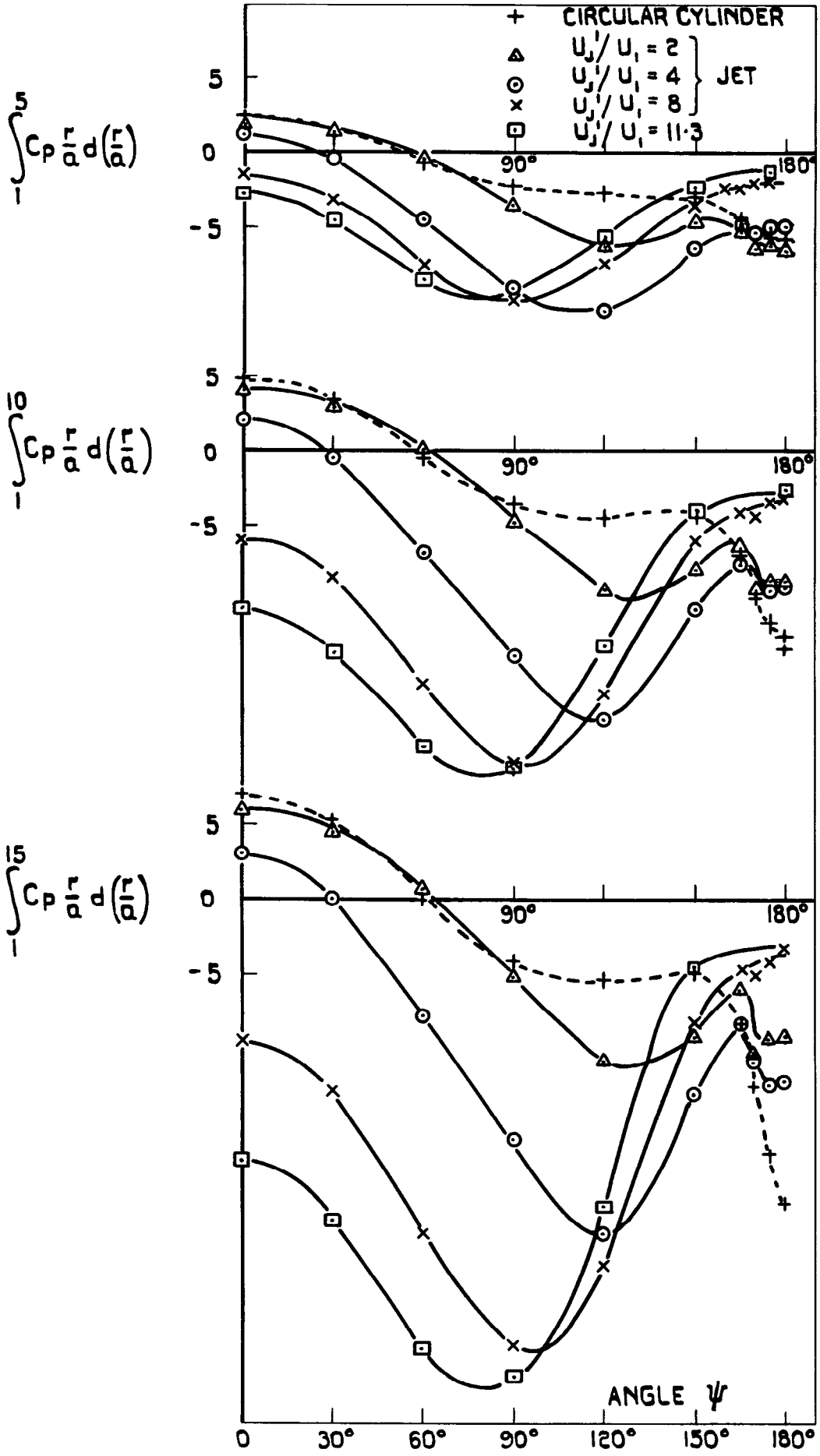

FIG. 12. DISTRIBUTION OF SURFACE PRESSURE FORCES AROUND THE JET AND CIRCULAR CYLINDER.

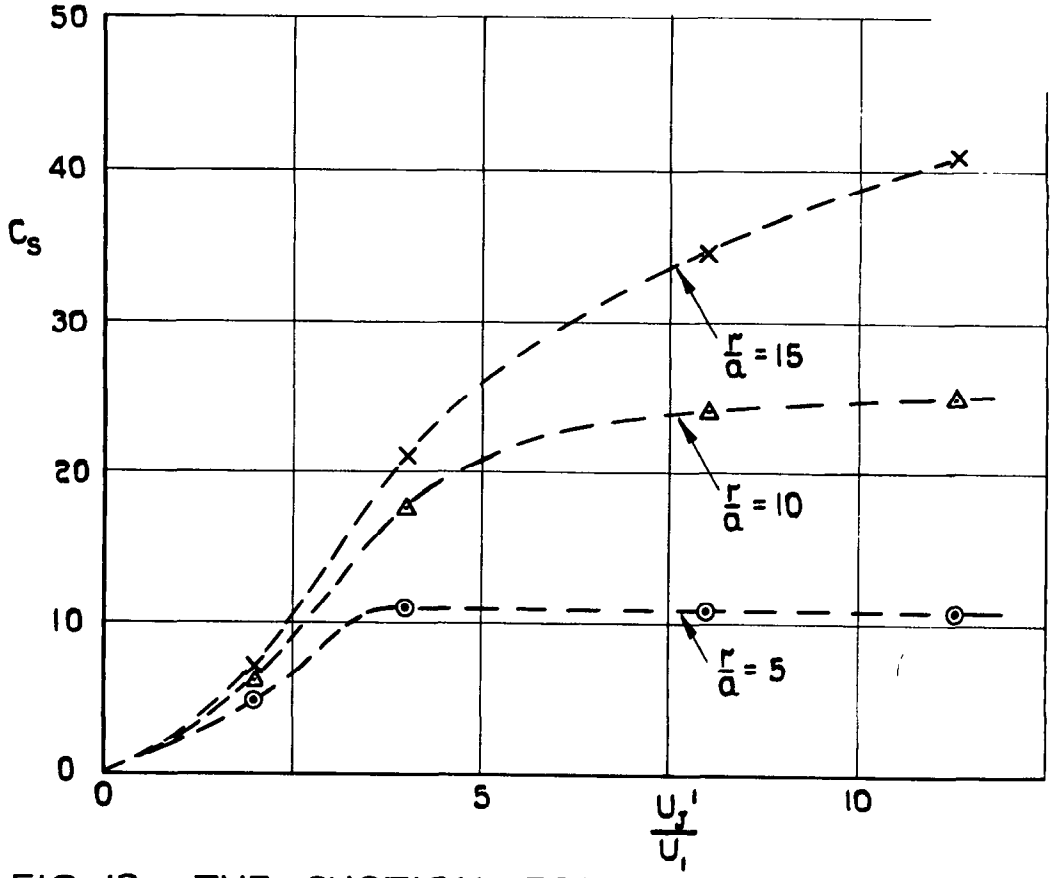

FIG. 13. THE SUCTION FORCE COEFFICIENTS.

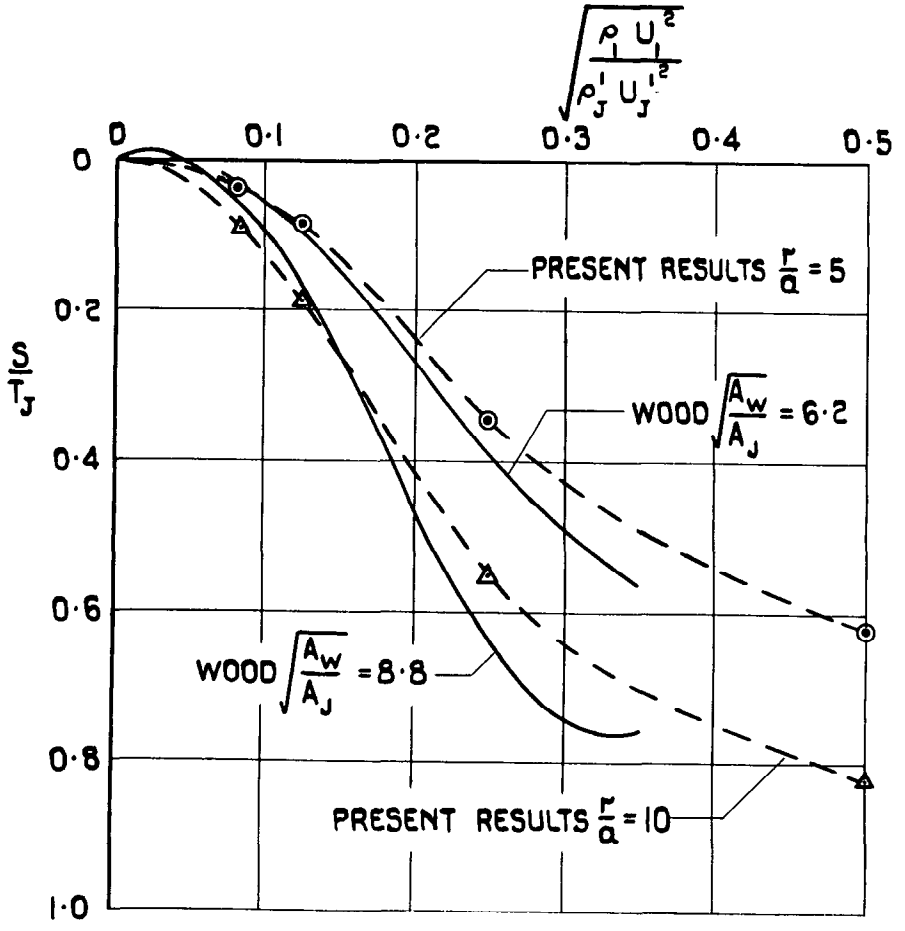

FIG. 14. COMPARISON BETWEEN THE PRESENT RESULTS AND DIRECT MEASUREMENTS OF LIFT LOSS.

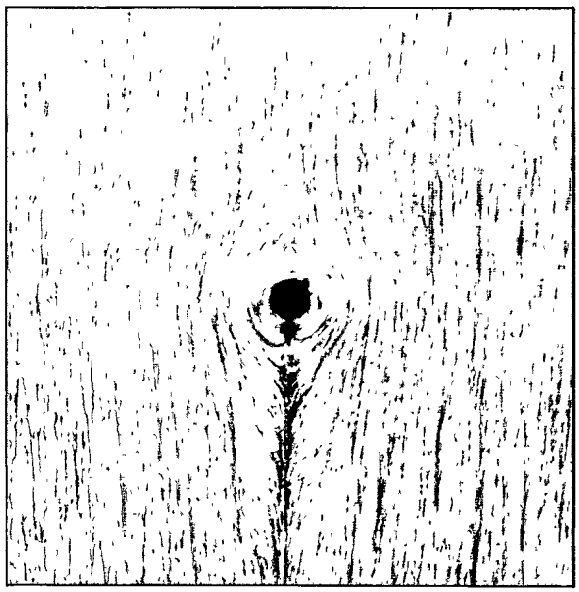

(a) Circular cylinder

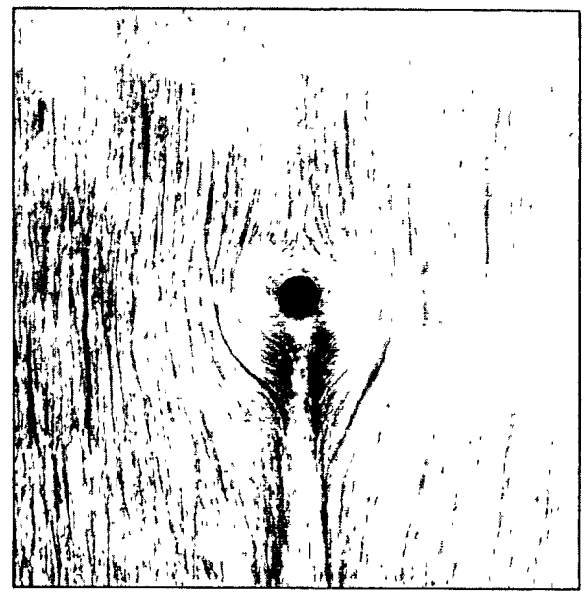

(b) $U_J'/U_1 = 2$

(c) $U_J'/U_1 = 4$

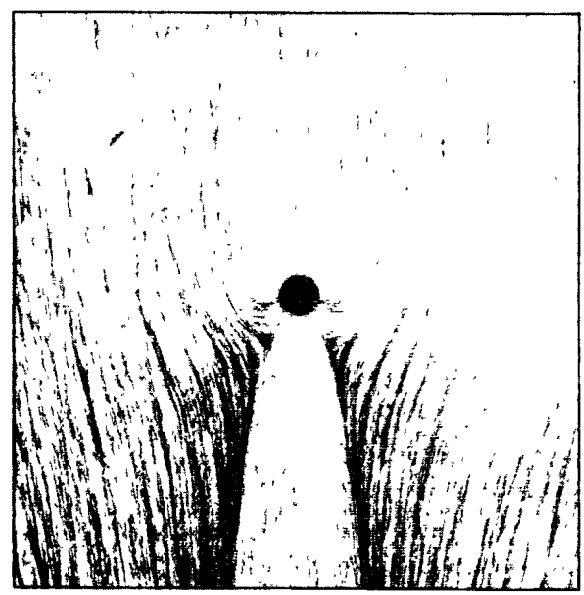

(d) $U_J'/U_1 = 8$

FIG. 15. FLOW PATTERNS ON THE WALL

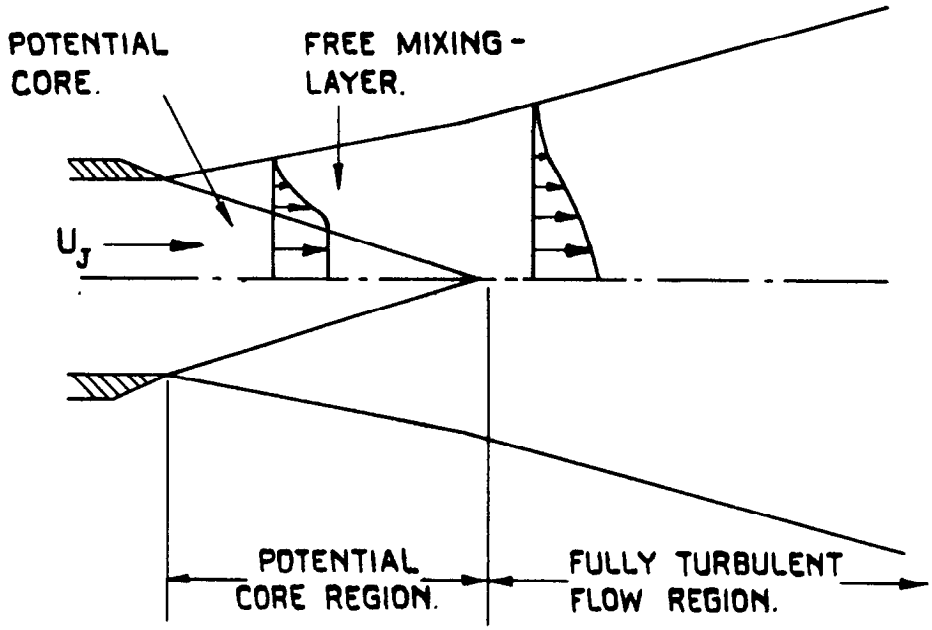

(a) SCHEMATIC REPRESENTATION OF JET FLOW.

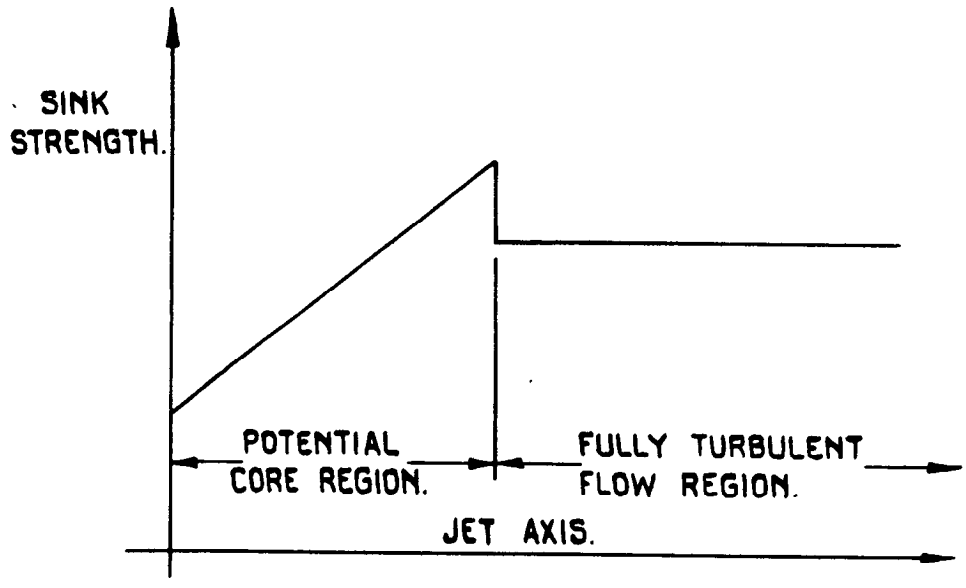

(b) LINE SINK DISTRIBUTION.

FIG. 16. REPRESENTATION OF ENTRAINMENT INTO AN AXI-SYMMETRIC JET BY A LINE DISTRIBUTION OF SINKS.

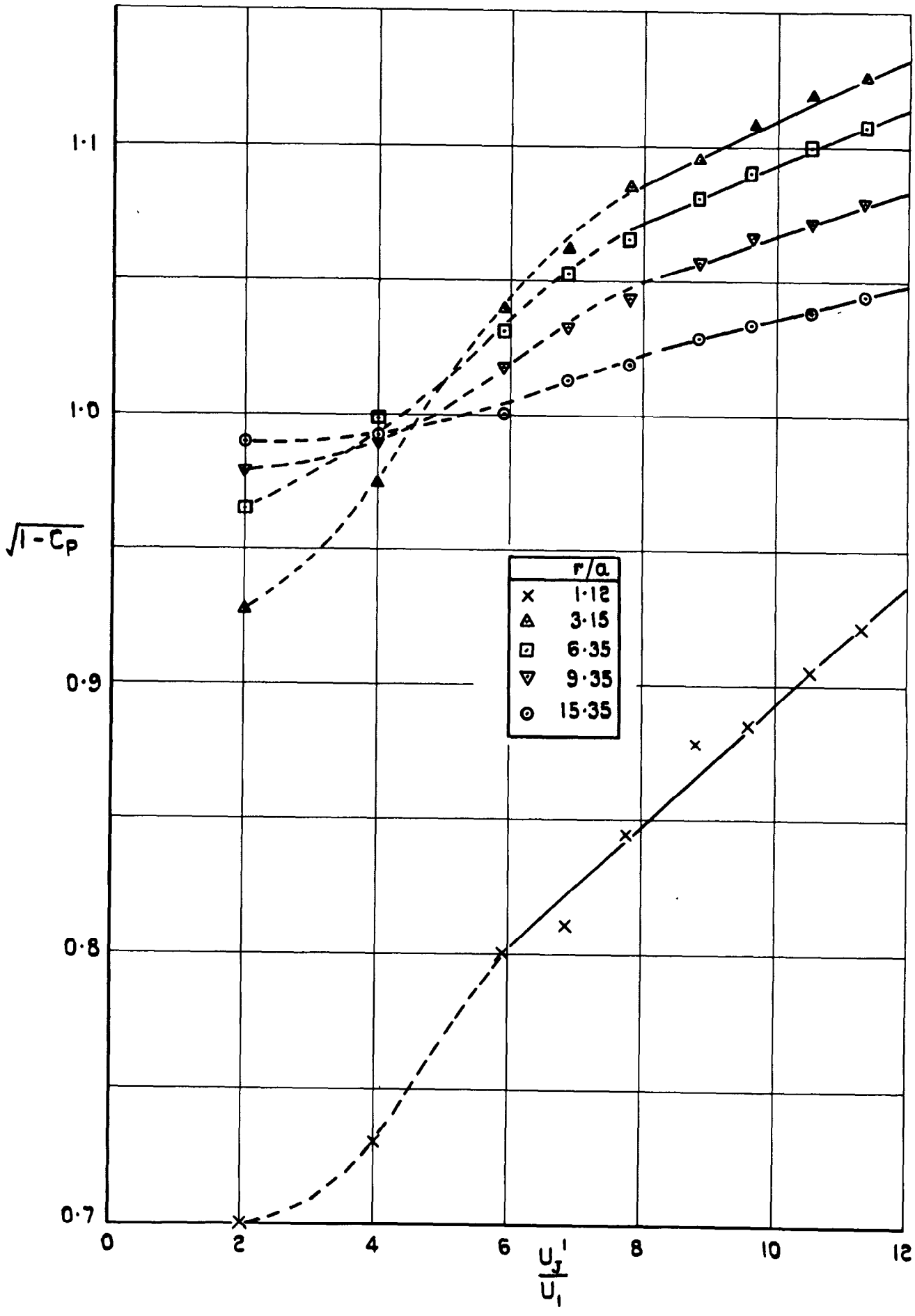

FIG. 17. STATIC PRESSURES UPSTREAM OF THE JET AT $\Psi = 0$.

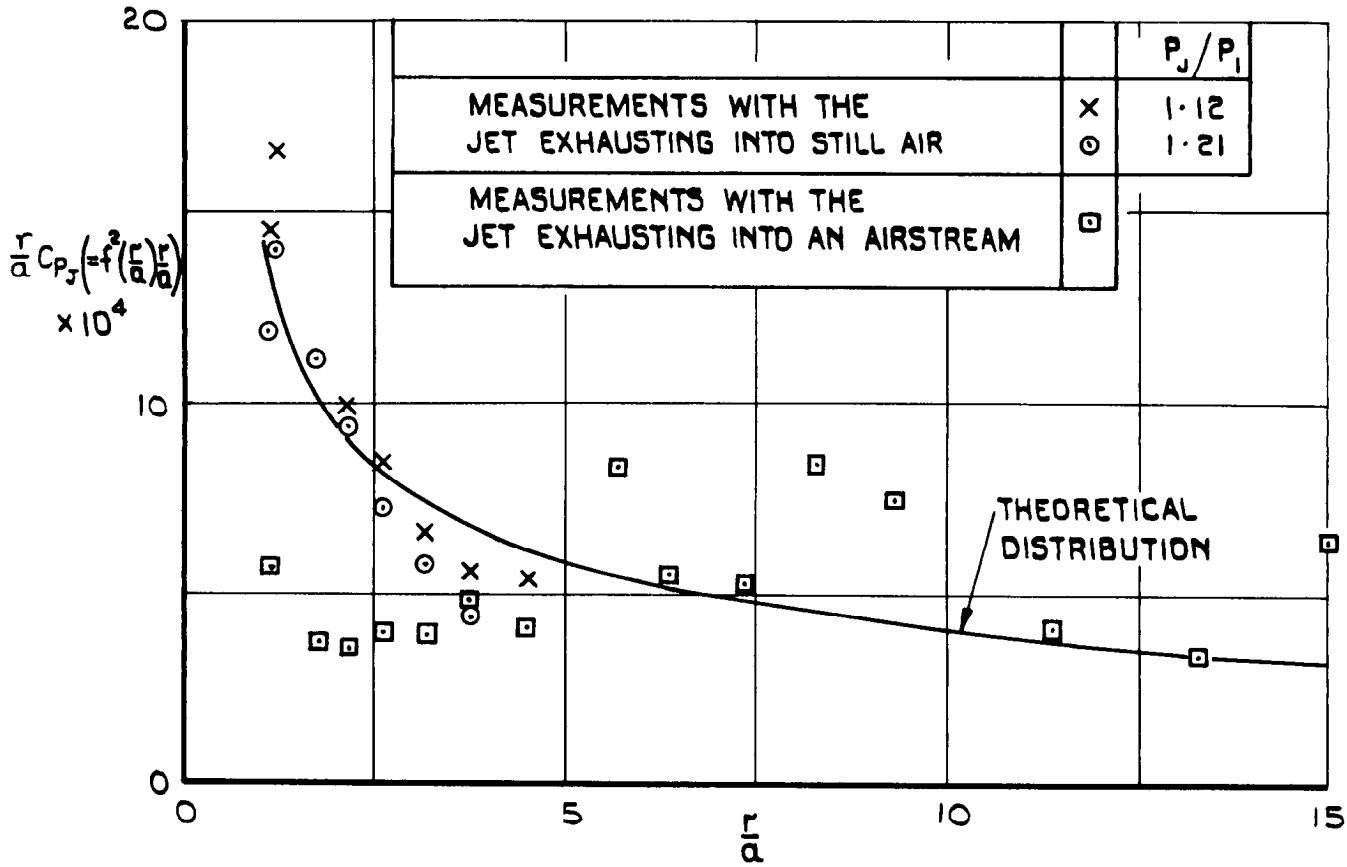

FIG. 18. A COMPARISON BETWEEN THE CALCULATED AND MEASURED STATIC PRESSURE INCREMENTS DUE TO ENTRAINMENT.

Printed in England for Her Majesty's Stationery Office by the Royal Aircraft Establishment, Farnborough. W.T.61. K.4.

A.R.C. C.P. No.822

533.6.048.2 :
532.529.3

THE STATIC PRESSURE DISTRIBUTION AROUND A CIRCULAR JET EXHAUSTING NORMALLY FROM A PLANE WALL INTO AN AIRSTREAM. Bradbury, L.J.S. and Wood, M.N.
August 1964.

Measurements have been made of the static pressure distribution on the wall around a circular jet exhausting normally from one wall of a wind tunnel into the mainstream flow through the tunnel. The measurements show the way in which the pressure distributions vary with the ratio of jet to free-stream velocity and also show the regions on the wall which contribute most to the overall suction force on the wall. These overall suction forces are shown to be of the right order of magnitude to account for the life loss observed on models of direct jet lift VTOL aircraft.

Theoretical work on the problem is briefly discussed and it is shown that a particularly simple model of the flow which has previously been suggested on a number of occasions is not really adequate.

A.R.C. C.P. No.822

533.6.048.2 :
532.529.3

THE STATIC PRESSURE DISTRIBUTION AROUND A CIRCULAR JET EXHAUSTING NORMALLY FROM A PLANE WALL INTO AN AIRSTREAM. Bradbury, L.J.S. and Wood, M.N.
August 1964.

Measurements have been made of the static pressure distribution on the wall around a circular jet exhausting normally from one wall of a wind tunnel into the mainstream flow through the tunnel. The measurements show the way in which the pressure distributions vary with the ratio of jet to free-stream velocity and also show the regions on the wall which contribute most to the overall suction force on the wall. These overall suction forces are shown to be of the right order of magnitude to account for the life loss observed on models of direct jet lift VTOL aircraft.

Theoretical work on the problem is briefly discussed and it is shown that a particularly simple model of the flow which has previously been suggested on a number of occasions is not really adequate.

A.R.C. C.P. No.822

533.6.048.2 :
532.529.3

THE STATIC PRESSURE DISTRIBUTION AROUND A CIRCULAR JET EXHAUSTING NORMALLY FROM A PLANE WALL INTO AN AIRSTREAM. Bradbury, L.J.S. and Wood, M.N.
August 1964.

Measurements have been made of the static pressure distribution on the wall around a circular jet exhausting normally from one wall of a wind tunnel into the mainstream flow through the tunnel. The measurements show the way in which the pressure distributions vary with the ratio of jet to free-stream velocity and also show the regions on the wall which contribute most to the overall suction force on the wall. These overall suction forces are shown to be of the right order of magnitude to account for the life loss observed on models of direct jet lift VTOL aircraft.

Theoretical work on the problem is briefly discussed and it is shown that a particularly simple model of the flow which has previously been suggested on a number of occasions is not really adequate.

Published by
HER MAJESTY'S STATIONERY OFFICE

To be purchased from
York House, Kingsway, London W.C.2
423 Oxford Street, London W.1
13A Castle Street, Edinburgh 2
109 St. Mary Street, Cardiff
39 King Street, Manchester 2
50 Fairfax Street, Bristol 1
35 Smallbrook, Ringway, Birmingham 5
80 Chichester Street, Belfast 1
or through any bookseller

C.P. No. 822

S.O. CODE No. 23-9016-22